work on other members of the Ta_2O_5–WO_3 system has confirmed this feature. The following description of the structure of $Ta_{15}Al_{\frac{1}{4}}W_{\frac{3}{4}}O_{40}$ is therefore based on the space group $P2$ and the atomic coordinates, listed in Table 3.

Tantalum, tungsten and aluminum atoms are statistically distributed in a close-packed hexagonal arrangement within sheets separated by 3·88 Å. The sheets are slightly puckered, the maximum displacement of a metal atom from the (001) plane being 0·08 Å. The oxygen atoms form coordination polyhedra about each metal atom in the form of either a distorted pentagonal bipyramid or octahedron and within the (001) planes these polyhedra share edges and corners. Extension of the structure along the [001] direction occurs by corner-sharing. Bond distances and angles for each polyhedron are listed in Table 4 together with e.s.d.'s. Observed and
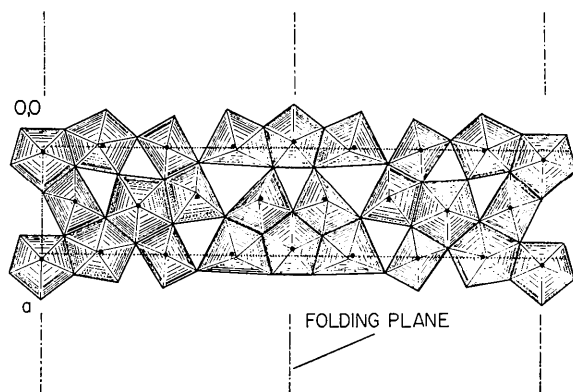

Fig. 2. A projection of the real structure of $Ta_{15}Al_{\frac{1}{4}}W_{\frac{3}{4}}O_{40}$ onto the (001) plane. Black dots represent metal atoms and shaded areas oxygen coordination polyhedra.

calculated structure factors are given in Table 5. A (001) projection of the structure is shown in Fig. 2.

The structure of $Ta_{15}Al_{\frac{1}{4}}W_{\frac{3}{4}}O_{40}$ differs from that of $Ta_{15}WO_{40\frac{1}{4}}$ only in that the partially occupied oxygen site O(21) of the latter structure is now completely empty in this present structure. There are thus two distortion planes per unit cell. These are related by a (020) mirror plane to form a doublet with an intraseparation distance of 7 Å. These doublets are repeated along the [010] direction at intervals of 29·2 Å ($=b$).

The most regular polyhedra are found midway between the (010) and (020) folding planes. The octahedron surrounding M(4) has metal–oxygen bond distances varying between 1·66 and 2·19 Å, oxygen–oxygen contact distances between 2·32 and 3·12 Å and a square planar arrangement of atoms within the (001) plane. The pentagonal bipyramid associated with M(7) is the most regular of this type of polyhedron, with metal–oxygen distances [2·07 (9) Å] averaging slightly greater than those in the M(4) octahedron [1·92 (6) Å]. Average oxygen–oxygen approach distances are the same for each type of polyhedron [2·72 (9) Å] and agree well with similar distances found in other studies (Stephenson & Roth, 1971a, b).

References

CROMER, D. T. & WABER, J. T. (1965). Acta Cryst. 18, 104.
DAUBEN, C. H. & TEMPLETON, D. H. (1955). Acta Cryst. 8, 841.
GELLER, S. (1961). Acta Cryst. 14, 1026.
STEPHENSON, N. C. & ROTH, R. S. (1971a). Acta Cryst. B27, 1010.
STEPHENSON, N. C. & ROTH, R. S. (1971b). Acta Cryst. B27, 1018.
SUZUKI, T. (1960). Acta Cryst. 13, 279.

Structural Systematics in the Binary System Ta_2O_5–WO_3. IV. The Structure of $Ta_{38}WO_{98}$

By N. C. Stephenson* and R. S. Roth

National Bureau of Standards, Washington, D.C. 20234. U.S.A.

The structure of the composition $Ta_{38}WO_{98}$ is described in terms of a 19 UO_3-type subcell unit containing 38 metal atoms and 95·5 oxygen atoms. The orthogonal unit cell has dimensions $a=6·188$, $b=69·57$, $c=3·880$ Å and the structure was solved in projection from the Patterson function utilizing photographically recorded data. Atomic positional and thermal parameters were refined by least-squares methods to a conventional R value of 0·118. The composition requires that the unit cell of the equilibrated compound be 429 UO_3-type subcells. As a result, the description of the structure in terms of an average 19 UO_3-type subcell unit introduces a splitting of certain atomic peaks. These effects are discussed.

Introduction

The composition $19Ta_2O_5.WO_3$ cannot be held in solid–liquid equilibrium like the previously described

compounds. Crystals are therefore difficult to prepare and thermal equilibration of the structure is very slow since both processes involve solid-state reactions. The crystal whose structure is described below was thermally equilibrated at 1605°C for 100 hours and can be considered to be close to the final equilibrium structure.

* Permanent address: School of Chemistry, University of New South Wales, Sydney, Australia.

The composition $19Ta_2O_5.WO_3$ has *not quite* the 19 UO_3-type subcell structure. The actual composition of 19 subcells would be $M_{22}O_{55}$ (11 subcell, Stephenson & Roth, 1971*d*) plus $M_{16}O_{40\frac{1}{2}}$ (8 subcell, Stephenson & Roth, 1971*b*) or $M_{38}O_{95\cdot5}$ *i.e.* $37Ta_2O_5.2WO_3$. The diffraction patterns of $19Ta_2O_5.WO_3$ can be satisfactorily indexed on the basis of a 19 UO_3-type subcell structure but the stoichiometry would require such a unit cell to contain $M_{38}O_{95\cdot487}$. The real unit cell of thermally equilibrated $19Ta_2O_5.WO_3$ has a *b* axis multiplicity of 429 and contains twenty-three 11 UO_3-type subcells together with twenty-two 8 UO_3-type subcells.

The structure described below has not quite reached the 19 UO_3-type subcell structure partially because of insufficient heat treatment and partially because of composition. Nevertheless, such a structure can be expected to provide information about the process by which the structure of any member of the series Ta_2O_5---$11Ta_2O_5.4WO_3$ undergoes a continuous change in reaching a final equilibrium state.

Experimental

Owing to the small departure from ideality, and a consequent uncertainty in the exact location of a diffracted beam, single-crystal X-ray data for the compound $19Ta_2O_5.WO_3$ were not collected using a diffractometer. Intensities were estimated from film packs using a calibrated strip prepared in the usual way from the crystal under examination. The equi-inclination Weissenberg method was used to collect data from a near-spherical crystal mounted about the *c* axis. Cu $K\alpha$ radiation was used and the data were processed (except absorption) using the *X-RAY* 67 program system (Stewart, 1967) and the NBS Univac 1108 computer. The crystal data are as follows: $Ta_{37}WO_{95\cdot487}$, $M = 8404\cdot3$; $a = 6\cdot188 \pm 0\cdot001$, $b =$

Table 1. *Positional and thermal atomic parameters*

Standard deviations are given in brackets and the form of the anisotropic thermal ellipsoid is $\exp[-(\beta_{11}h^2 + \beta_{22}k^2 + 2\beta_{12}hk)]$. Atoms O(20) to O(29) have *z* parameters of $\frac{1}{2}$; the remaining atoms have *z* parameters of zero. Bracketed atoms are doublets and each atom O(14) to O(19) has a population parameter of 0·5. The population parameters for O(12) and O(13) are 0·125 and 0·750 respectively.

	x/a	y/b	$\beta_{11} \times 10^4$ or B	$\beta_{22} \times 10^5$	$\beta_{12} \times 10^5$
M(1)	0·0641 (44)	0·04939 (28)	141 (54)	2 (2)	−84 (36)
M(2)	0·0445 (42)	0·10594 (30)	16 (37)	12 (38)	34 (28)
M(3)	0·0583 (37)	0·16014 (19)	73 (53)	3 (2)	29 (26)
M(4)	0·1582 (31)	0·21044 (28)	17 (26)	6 (2)	−42 (22)
M(5)	0·5354 (37)	0·02765 (23)	−108 (29)	3 (3)	7 (22)
M(6)	0·5176 (33)	0·08061 (19)	−18 (29)	−4 (1)	−1 (20)
M(7)	0·6263 (48)	0·12963 (29)	21 (41)	6 (3)	−32 (31)
M(8)	0·5783 (39)	0·18365 (16)	53 (38)	0 (2)	13 (24)
M(9)	0·5749 (29)	0·23929 (21)	1 (26)	1 (2)	−17 (22)
M(10)	0·0000	0·0000	−94 (35)	−4 (4)	0
O(1)	0·872 (41)	0·0277 (37)	−2·1 (4·3)		
O(2)	0·407 (54)	0·0529 (43)	0·2 (4·1)		
O(3)	0·642 (43)	0·0000	−1·7 (5·4)		
O(4)	0·162 (46)	0·0796 (46)	−0·1 (5·0)		
O(5)	0·366 (55)	0·1109 (46)	1·5 (6·4)		
O(6)	0·712 (37)	0·1572 (39)	−0·7 (4·8)		
O(7)	0·234 (33)	0·2360 (35)	−0·6 (3·6)		
O(8)	0·504 (45)	0·2104 (43)	0·9 (5·0)		
O(9)	0·980 (41)	0·1294 (34)	0·3 (4·8)		
O(10)	0·793 (29)	0·0984 (42)	−0·9 (4·3)		
O(11)	0·900 (31)	0·1894 (36)	−0·9 (3·8)		
O(12)	0·250 (55)	0·0089 (5)	−0·8 (2·1)		
O(13)	0·288 (44)	0·0185 (54)	−1·6 (5·1)		
O(14)	0·815 (44)	0·0626 (54)	−1·2 (5·4)		
O(15)	0·869 (81)	0·0760 (79)	−1·2 (5·1)		
O(16)	0·288 (42)	0·1362 (43)	−2·1 (4·8)		
O(17)	0·380 (46)	0·1533 (58)	−0·6 (3·4)		
O(18)	0·790 (47)	0·2123 (61)	−0·5 (4·1)		
O(19)	0·892 (41)	0·2307 (58)	−0·9 (3·8)		
O(20)	0·057	0·0495	0·2		
O(21)	0·049	0·1055	0·2		
O(22)	0·057	0·1602	0·2		
O(23)	0·158	0·2107	0·2		
O(24)	0·530	0·0274	0·2		
O(25)	0·514	0·0808	0·2		
O(26)	0·620	0·1294	0·2		
O(27)	0·582	0·1832	0·2		
O(28)	0·572	0·2392	0·2		
O(29)	0·000	0·0000	0·2		

69·570±0·001, $c=3·880±0·001$Å, $V_o=1670$Å^3, $Z=1$, $D_c=8·36$ g.cm^{-3}, $\mu R=1·95$. Unit-cell dimensions were obtained using a Philips powder diffractometer with Cu $K\alpha$ radiation. Atomic scattering curves and computer programs were the same as described previously (Stephenson & Roth, 1971*a*).

Determination and refinement of the structure

The principal structural features were determined by projection along the short *c* axis. The Laue symmetry and systematic absences in spectra indicated a *C*-centered orthorhombic space group so that the plane group for the (001) projection is either *Cmm* or *Cm*. It was possible to interpret the Patterson function with the latter plane group and the positions of the metal atoms were determined from superposition maps using the minimum-function approach (Buerger, 1959). Most atoms are located in the (001) planes since the intensity distributions on zero and upper-level Weissenberg photographs were visually identical.

Table 2. *Observed and calculated structure factors*

Unobserved data are marked with L.

H	K		FO	FC
0	2	L	13	21
0	4	L	19	2
0	6	L	24	29
0	8	L	28	45
0	10	L	31	38
0	12	L	34	16
0	16	L	40	44
0	18	L	43	30
0	20	L	45	6
0	22	L	48	23
0	24		442	410
0	26	L	53	62
0	28	L	55	6
0	30	L	58	66
0	32	L	60	34
0	34	L	63	65
0	36	L	66	17
0	38		1581	1994
0	40	L	71	62
0	42	L	73	105
0	44	L	76	60
0	46	L	78	32
0	48	L	81	149
0	50	L	83	107
0	52		501	513
0	54	L	88	66
0	56	L	89	97
0	58	L	91	54
0	60	L	92	20
0	62		698	711
0	64	L	93	114
0	66	L	93	102
0	68	L	92	88
0	70	L	90	102
0	72	L	88	2
0	74	L	85	107
0	76		900	838
1	1	L	33	18
1	3	L	34	49
1	9	L	38	28
1	11	L	39	68
1	13	L	41	51
1	15	L	44	61
1	17		313	320
1	19		1539	2100
1	21		202	248
1	23	L	52	64
1	25	L	55	64
1	27	L	57	52
1	29	L	59	15
1	31		473	426
1	33		585	580
1	35		94	89
1	37	L	69	63
1	39	L	72	48
1	41		105	94
1	43		606	537
1	45		194	189
1	47	L	81	83
1	49	L	84	96
1	51	L	86	65
1	53	L	88	78
1	55		270	247
1	57		985	1155
1	59	L	92	121
1	61	L	93	93
1	63	L	93	115
1	65	L	93	26
1	67		226	176
1	69		287	307
1	71		697	591
1	73	L	85	85
1	75	L	82	99
1	79		165	138
1	81		568	581
2	0		1501	1922
2	2		631	557
2	4	L	49	50
2	6	L	49	65
2	8	L	50	26
2	10		145	128
2	12		527	451
2	14		488	445
2	16	L	55	89
2	18	L	56	41
2	20	L	58	28
2	22		85	70
2	24		351	330
2	26		512	441
2	28	L	65	42
2	30	L	68	69
2	32	L	70	42
2	34		144	141
2	36		566	611
2	38		1206	1438
2	40		324	318
2	42	L	80	68
2	44	L	83	94
2	46	L	85	30
2	48	L	87	15
2	50		344	333
2	52		723	667
2	54	L	91	89
2	56	L	92	67
2	58	L	93	89
2	60	L	93	126
2	62		543	497
2	64		292	231
2	66	L	90	95
2	68	L	88	70
2	70	L	86	76
2	74		527	449
2	76		845	686
2	78		199	186
3	1	L	63	15
3	3		155	142
3	5		509	455
3	7		785	752
3	9		533	267
3	11	L	65	18
3	13	L	66	92
3	15		201	195
3	17		736	775
3	19		1436	1511
3	21		634	535
3	23		102	44
3	25	L	73	76
3	27	L	75	24
3	29		243	245
3	31		497	598
3	33		580	706
3	35		142	191
3	37	L	83	66
3	39	L	85	68
3	41	L	87	59
3	43		125	157
3	45		476	491
3	47	L	91	62
3	49	L	92	64
3	51	L	93	60
3	53		264	228
3	55		793	691
3	57		1019	606
3	59		357	276
3	61	L	90	94
3	63	L	89	100
3	65	L	86	40
3	67	L	84	85
3	69		378	385
3	71		605	601
3	73		125	157
4	0		1130	992
4	2		640	585
4	4		134	140
4	6	L	78	98
4	8	L	78	19
4	10		387	340
4	12		516	564
4	14		642	711
4	16		256	281
4	18	L	81	33
4	20	L	82	56
4	22	L	83	124
4	24		294	319
4	26		333	412
4	28		125	174
4	30	L	88	46
4	32	L	89	78
4	34		221	259
4	36		576	647
4	38		759	729
4	40		346	331
4	42	L	93	68
4	44	L	93	107
4	46	L	93	22
4	48		294	278
4	50		472	461
4	52		698	716
4	54		255	247
4	56	L	88	93
4	58	L	86	127
4	60	L	84	109
4	62	L	81	108
4	64		245	259
4	66	L	73	76
4	68	L	69	52
4	72		236	267
4	74		452	525
4	76		327	365
5	1	L	90	53
5	3		285	294
5	5		612	552
5	7		461	417
5	9		405	363
5	11	L	90	51
5	13	L	91	96
5	15		258	230
5	17		687	636
5	19		771	610
5	21		453	444
5	23	L	92	94
5	25	L	93	114
5	27	L	93	82
5	29		438	428
5	31		458	400
5	33		781	744
5	35		322	323
5	37	L	92	65
5	39	L	91	93
5	41	L	91	87
5	43		179	176
5	45		265	278
5	47	L	86	134
5	49	L	84	54
5	53		276	316
5	55		614	619
5	57		415	411
5	59		241	254
5	61	L	65	59
5	63	L	60	112
5	65	L	55	90
5	67		188	270
6	0		570	519
6	2		506	423
6	4	L	92	136
6	6	L	92	103
6	8	L	92	92
6	10		451	447
6	12		318	253
6	14		819	713
6	16		465	418
6	18	L	90	81
6	20	L	90	97
6	22		380	342
6	24		562	489
6	26		276	252
6	28		301	289
6	30	L	85	73
6	32	L	84	100
6	34		321	271
6	36		586	514
6	38		449	452
6	40		345	289
6	42	L	74	86
6	44	L	72	108
6	46		138	136
6	48		493	440
6	50		124	156
6	52		632	655
6	54		329	337
7	1	L	76	113
7	3		404	426
7	5		549	514
7	7	L	75	69
7	9		213	285
7	11	L	74	81
7	15		179	162
7	17		338	364
7	19		376	410
7	21		220	328
7	23	L	68	90
7	25	L	66	100
7	27	L	64	116
7	29		343	367
7	31	L	60	104
7	33		446	566
7	35		298	391

The positional and isotropic thermal parameters of each metal atom in the asymmetric unit were refined by least-squares methods to a conventional R value of 0·168. The weighting scheme used in these cycles was slightly different from that used with diffractometer data since no reliable standard deviations in structure factor amplitudes were known. It was necessary to minimize the effect of errors due to extinction and the weights were calculated according to the scheme

$$\sqrt{w}=\frac{Q_1}{\max\,(Q_2F,\,Q_3)}$$

with $Q_1=51·2$, $Q_2=1$ and $Q_3=512·0$.

Oxygen atoms were located by difference Fourier syntheses, which also indicated thermal anisotropy for the metal atoms. Atomic parameters were refined by least-squares cycles, based on F, to the values listed in Table 1. Oxygen atoms that projected close to metal atoms were not varied in the least-squares cycles and small, positive isotropic thermal parameters were assigned to them. The final agreement factor R_1, was 0·118.

Table 2 lists observed and calculated structure factors. Bond distances and angles, together with their estimated standard deviations (e.s.d's) are given in Table 3.

Table 3. *Selected bond distances* (Å) *and angles* (°) *for the compound* $Ta_{38}WO_{98}$

Standard deviations are given together with frequency of occurrence (second parentheses). * and † refer to coordinates of the midpoint of the oxygen doublet and symmetry related atom $\bar{x}$, $\frac{1}{2}-y$, z respectively. The prime refers to symmetry related atom x, $\bar{y}$, z.

M(1) Pentagonal bipyramid

M(1) —O(1)	1·92 (26) (1)
—O(2)	2·14 (34) (1)
—O(4)	2·19 (32) (1)
—O(13)	2·56 (35) (1)
—O(14)	1·95 (31) (1)
—O(20)	1·94 (20) (2)
O(1)—O(14)	2·69 (45) (1)
O(14)—O(4)	2·38 (41) (1)
O(4)—O(2)	2·40 (44) (1)
O(2)—O(13)	2·50 (48) (1)
O(13)—O(1)	2·65 (38) (1)
O(20)—O(1)	2·72 (30) (2)
—O(2)	2·92 (34) (2)
—O(4)	2·93 (35) (2)
—O(13)	3·23 (29) (2)
—O(14)	2·72 (32) (2)
O(1)—O(14)—O(4)	105 (14)
O(14)—O(4)—O(2)	106 (17)
O(4)—O(2)—O(13)	123 (17)
O(2)—O(13)—O(1)	93 (15)
O(13)—O(1)—O(14)	112 (13)

M(2) Octahedron

M(2) —O(4)	1·97 (32) (1)
—O(5)	2·02 (34) (1)
—O(9)	1·68 (24) (1)
—O(10)	1·64 (20) (1)

Table 3 (*cont.*)

M(2)—O(21)	1·94 (20) (2)
O(4)——O(5)	2·52 (45) (1)
O(5)——O(9)	2·71 (42) (1)
O(9)——O(10)	2·45 (36) (1)
O(10)—O(4)	2·63 (36) (1)
O(21)—O(4)	2·74 (33) (2)
—O(5)	2·78 (33) (2)
—O(9)	2·59 (28) (2)
—O(10)	2·55 (24) (2)
O(4)—O(5)——O(9)	88 (13)
O(5)—O(9)——O(10)	90 (11)
O(9)—O(10)——O(4)	92 (11)
O(10)—O(4)——O(5)	90 (14)

M(3) Octahedron

M(3) —O(6)	2·15 (23) (1)
—O(9)	2·19 (24) (1)
—O(11)	2·25 (24) (1)
—O(17)	2·05 (29) (1)
—O(22)	1·94 (20) (2)
O(6)——O(9)	2·55 (35) (1)
O(9)——O(17)	2·98 (41) (1)
O(17)—O(11)	3·78 (38) (1)
O(11)—O(6)	2·52 (36) (1)
O(22)—O(6)	2·89 (29) (2)
—O(9)	2·93 (31) (2)
—O(11)	2·97 (32) (2)
—O(17)	2·83 (31) (2)
O(6)——O(9)——O(17)	97 (12)
O(9)——O(17)—O(11)	78 (11)
O(11)—O(6)——O(9)	112 (11)
O(17)—O(11)—O(6)	73 (12)

M(4) Octahedron

M(4) —O(7)	1·84 (24) (1)
—O(8)	2·14 (28) (1)
—O(11)	2·17 (22) (1)
—O(18)*	2·07 (23) (1)
—O(23)	1·94 (20) (2)
O(7)——O(8)	2·44 (37) (1)
O(8)——O(11)	2·85 (35) (1)

Table 3 (*cont.*)

O(11)—O(18)*	2·80 (36) (1)
O(18)—O(7)	2·54 (34) (1)
O(23)—O(7)	2·66 (29) (2)
—O(8)	2·89 (31) (2)
—O(11)	2·92 (30) (2)
—O(18)*	2·94 (31) (2)
O(7)——O(8)——O(11)	75 (12)
O(8)——O(11)—O(18)*	75 (11)
O(11)—O(18)*-O(7)	105 (12)
O(18)*-O(7)——O(8)	105 (12)

M(5) Octahedron

M(5) —O(1)	2·08 (26) (1)
—O(2)	1·93 (31) (1)
—O(3)	2·03 (09) (1)
—O(13)	1·66 (29) (1)
—O(24)	1·94 (20) (2)
O(1)——O(2)	3·37 (41) (1)
O(2)——O(13)	2·50 (48) (1)
O(13)—O(3)	2·54 (38) (1)
O(3)——O(1)	2·40 (30) (1)
O(24)—O(1)	2·87 (30) (2)
—O(2)	2·74 (32) (2)
—O(3)	2·81 (26) (2)
—O(13)	2·53 (27) (2)
O(1)——O(2)——O(13)	76 (11)
O(2)——O(13)—O(3)	103 (13)
O(13)—O(3)——O(1)	96 (10)
O(3)——O(1)——O(2)	85 (10)

M(6) Pentagonal bipyramid

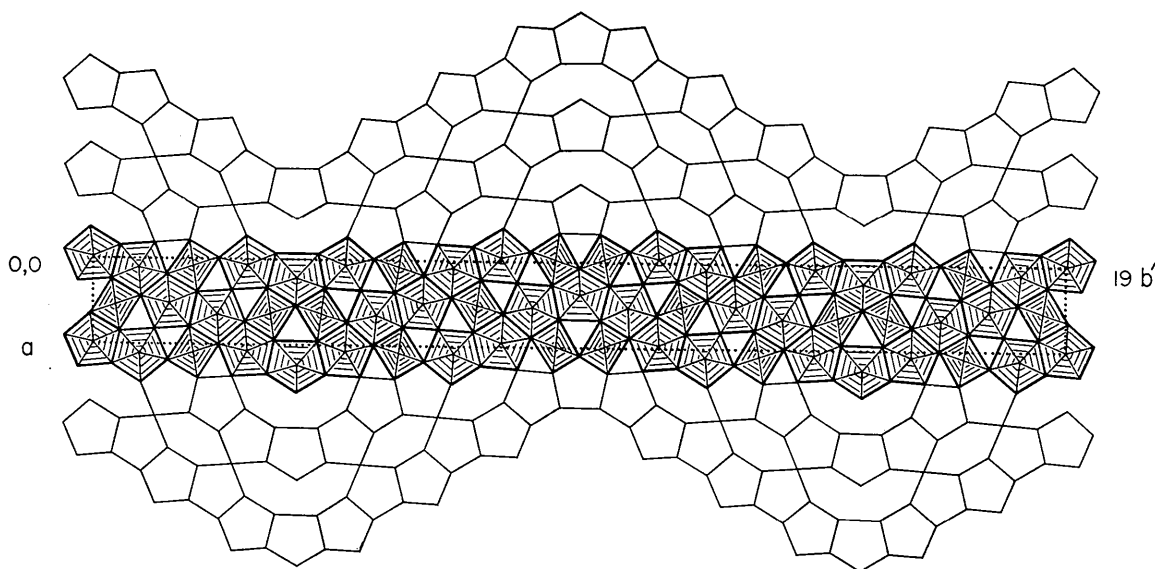| M(6) —O(2)	2·05 (30) (1)
—O(4)	2·20 (29) (1)
—O(5)	2·31 (32) (1)
—O(10)	2·11 (23) (1)
—O(14)	2·08 (30) (1)
—O(25)	1·94 (20) (2)
O(2)——O(4)	2·40 (44) (1)
O(4)——O(5)	2·52 (45) (1)
O(5)——O(10)	2·78 (39) (1)
O(10)—O(14)	2·26 (48) (1)

Fig. 1. The ideal structure of 19 UO_3-type subcells. The contents of the unit cell are M_3O_{100}, where M represents a metal atom, and the structure is made up of chains of fused pentagons which are 6 and 8 pentagons long in the linear sections.

Table 3 (*cont.*)

O(14)—O(2)	2·66 (44) (1)
O(25)—O(2)	2·82 (33) (2)
—O(4)	2·92 (31) (2)
—O(5)	3·00 (36) (2)
—O(10)	2·87 (29) (2)
—O(14)	2·86 (32) (2)
O(2)—O(4)—O(5)	111 (15)
O(4)—O(5)—O(10)	102 (14)
O(5)—O(10)—O(14)	111 (13)
O(10)—O(14)—O(2)	107 (14)
O(14)—O(2)—O(4)	109 (15)

M(7) Pentagonal bipyramid

M(7) —O(5)	2·07 (33) (1)
—O(6)	1·99 (27) (1)
—O(9)	2·19 (26) (1)
—O(10)	2·41 (28) (1)
—O(17)	2·24 (36) (1)
—O(26)	1·94 (20) (2)
O(5)—O(17)	2·95 (52) (1)
O(17)—O(6)	2·17 (37) (1)
O(6)—O(9)	2·55 (35) (1)
O(9)—O(10)	2·45 (36) (1)
O(10)—O(5)	2·78 (39) (1)
O(26)—O(5)	2·81 (34) (2)
—O(6)	2·80 (32) (2)
—O(9)	2·95 (30) (2)
—O(10)	3·09 (34) (2)
—O(17)	3·00 (37) (2)
O(5)—O(17)—O(6)	99 (16)
O(17)—O(6)—O(9)	123 (17)
O(6)—O(9)—O(10)	111 (12)
O(9)—O(10)—O(5)	100 (13)
O(10)—O(5)—O(17)	107 (13)

M(8) Octahedron

M(8) —O(6)	2·01 (27) (1)
—O(8)	1·92 (30) (1)
—O(11)	2·03 (20) (1)
—O(17)	2·44 (38) (1)
—O(27)	1·94 (20) (2)
O(6)—O(17)	2·17 (37) (1)
O(17)—O(8)	3·90 (38) (1)
O(8)—O(11)	2·85 (35) (1)
O(11)—O(6)	2·52 (36) (1)
O(27)—O(6)	2·77 (31) (2)
—O(8)	2·75 (32) (2)
—O(11)	2·80 (26) (2)
—O(17)	3·11 (40) (2)
O(6)—O(17)—O(8)	69 (16)
O(17)—O(8)—O(11)	75 (16)
O(8)—O(11)—O(6)	83 (10)
O(11)—O(6)—O(17)	124 (17)

M(9) Octahedron

M(9) —O(7)	2·12 (21) (1)
—O(7)†	1·98 (24) (1)
—O(8)	2·06 (30) (1)
—O(18)*	1·90 (28) (1)
—O(28)	1·94 (20) (2)
O(7)—O(7)†	3·57 (35) (1)
O(7)†—O(18)	2·73 (33) (1)
O(18)—O(8)	2·82 (33) (1)
O(8)—O(7)	2·44 (37) (1)
O(28)—O(7)	2·86 (27) (2)
—O(7)†	2·77 (32) (2)
—O(8)	2·82 (33) (2)
—O(18)*	2·72 (35) (2)
O(7)†—O(18)—O(8)	79 (17)
O(18)—O(8)—O(7)	107 (16)
O(8)—O(7)—O(7)†	79 (18)
O(7)—O(7)†—O(18)	95 (17)

Table 3 (*cont.*)

M(10) Pentagonal bipyramid

M(10) —O(1)	2·08 (26) (2)
—O(3)	2·22 (27) (1)
—O(13)	2·20 (31) (2)
—O(29)	1·94 (20) (2)
O(1)—O(3)	2·40 (30) (2)
O(1)—O(13)	2·65 (38) (2)
O(13)—O(13′)	2·57 (53) (1)
O(29)—O(1)	2·85 (31) (4)
—O(3)	2·95 (31) (2)
—O(13)	2·93 (34) (4)
O(1)—O(3)—O(1′)	107 (13) (1)
O(3)—O(1)—O(13)	112 (13) (2)
O(1)—O(13)—O(13′)	104 (14) (2)

M(10) Octahedron

M(10) —O(1)	2·08 (26) (2)
—O(3)	2·22 (27) (1)
—O(12)	1·67 (32) (1)
—O(29)	1·94 (20) (2)
O(1)—O(3)	2·40 (30) (2)
O(1)—O(12)	3·46 (35) (1)
O(1′)—O(12)	2·68 (39) (1)
O(29)—O(1)	2·85 (31) (4)
—O(3)	2·95 (31) (2)
—O(12)	2·56 (29) (2)
O(1)—O(3)—O(1′)	107 (13)
O(3)—O(1)—O(12)	97 (11)
O(1)—O(12)—O(1′)	77 (10)
O(12)—O(1′)—O(3)	79 (12)

Description and discussion of the structure

The 19 UO_3-type subcell structure can be considered as a combination of the basic 8 and 11 UO_3-type subcell structures. The chain lengths in these cases are 6 and 8 pentagons and the ideal structure is shown in Fig. 1. This unit cell contains 38 metal and 100 oxygen atoms, whereas the real unit cell of the 19 UO_3-type subcell structure contains 38 metal and $95\frac{1}{2}$ oxygen atoms. There are thus $4\frac{1}{2}$ distortion planes per unit cell.

Four of the distortion planes can be immediately located. They are associated with an oxygen atom which would occur at (0·30, 0·18, 0·00) in the ideal structure but is completely missing in the real structure. Small movements in positions of neighboring oxygen atoms give metal atoms M(3), M(4) and M(8) distorted octahedral environments, whereas in the ideal structure the former two would each be surrounded by a pentagonal bipyramid of oxygen atoms. The general position in plane group Cm is fourfold and therefore these four distortion planes occur at d_1, d_2, d_3 and d_4 as shown in Fig. 2.

The disposition of these four distortion planes is important. They occur in doublets. No association of distortion planes is possible in the compound $11Ta_2O_5.4WO_3$. In the compounds $15Ta_2O_5.2WO_3$ and $45Ta_2O_5.Al_2O_3.2WO_3$ the distribution of distortion planes along the b axis depends on the plane group (Stephenson & Roth, 1971a, b, c). A distribution involving doublets was inferred for the latter two compounds but with the present investigation there is
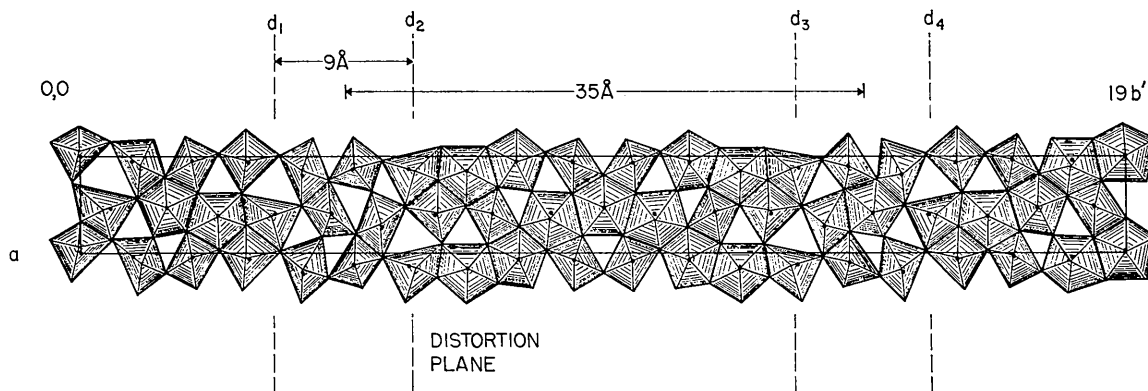
Fig. 2. The real structure of 19 UO_3-type subcells in the system $Ta_2O_5-WO_3$. The contents of the unit cell depicted here are $M_{38}O_{95}$ and distortion planes occur where reductions in coordination numbers have occurred for certain metal atoms. Four distortion planes are shown, related by the symmetry elements of plane group Cm, and they occur in doublets each separated by approximately 35 Å. Black dots represent oxygen atoms and shaded areas represent oxygen coordination polyhedra.

no doubt that distortion planes associate as doublets.

The remaining distortion plane can be identified with oxygen atoms O(12) and O(13) constituting a doublet in exactly the same position as O(17) and O(18) in the compound $11Ta_2O_5.4WO_3$. This distortion plane occurs every two unit cells so that metal atom M(10) has pentagonal bipyramidal coordination and distorted octahedral coordination in the ratio 3:1. The area of the structure depicted in Fig. 2 is therefore, on the average, one half a unit cell.

The consequence of the compound $19Ta_2O_5.WO_3$ not being fully equilibrated thermally, and also being slightly off composition, appears in the Fourier syntheses. Oxygen atoms in the (001) plane, which occur where two pentagons share a corner, appear as doublets and the line of centers of each doublet is perpendicular to the line of centers of the pentagon pair involved in the corner sharing. The movement of a corner shared oxygen atom along such a line of centers e.g. O(14)–O(15), Fig. 3, tends to transform the neighboring octahedra e.g. M(2) and M(5) into pentagonal bipyramids. The converse is also true: the superposition of distorted octahedra and pentagonal bipyramids will cause the observed splitting. The splitting of these corner-shared oxygen atoms is therefore a result of an oxygen framework that is not yet periodic along the [010] direction. Oxygen atoms are still moving into their equilibrium positions and they do so, locally, in sheets which move perpendicular to the b axis.

The coordinated movements of atoms, in sheets, has been postulated by Andersson & Wadsley (1966) to explain the formation and subsequent migration of shear planes within a crystal. The local movement of sheets of atoms as demonstrated above, bears an
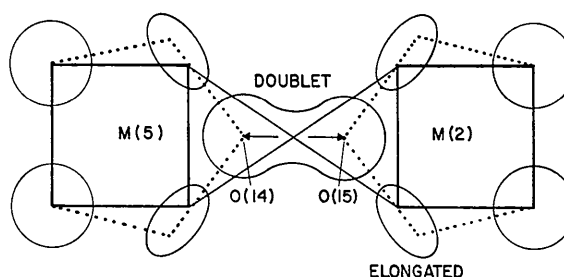

Fig. 3. The effect of superimposing two square coordinated metal atoms [M(5) and M(2) in heavy lines] and two pentagonally coordinated metal atoms [M(5) and M(2) in dotted lines]. Some atoms remain spherical, others elongate and the atom along the line of centers is split into two (or three) weaker peaks.

analogous relationship to the migration of distortion planes through a crystal during thermal equilibration and this is discussed in more detail in the next paper (Stephenson & Roth, 1971d).

References

ANDERSSON, S. & WADSLEY, A. D. (1966). Nature, Lond. 211, 581.

BUERGER, M. J. (1959). Vector Space and its Application in Crystal Structure Investigation. New York: John Wiley.

STEPHENSON, N. C. & ROTH, R. S. (1971a). Acta Cryst. B27, 1010.

STEPHENSON, N. C. & ROTH, R. S. (1971b). Acta Cryst. B27, 1018.

STEPHENSON, N. C. & ROTH, R. S. (1971c). Acta Cryst. B27, 1025.

STEPHENSON, N. C. & ROTH, R. S. (1971d). Acta Cryst. B27, 1037.

STEWART, J. M. (1967). Technical Report 67–58, Computer Science Center, Univ. of Maryland.